Karlsruhe Institute of Technology

# Estimation of swelling stresses from crack-terminating angles

P. Hettich, K. G. Schell, G. Rizzi, S. Wagner, T. Fett

KIT SCIENTIFIC WORKING PAPERS **119**

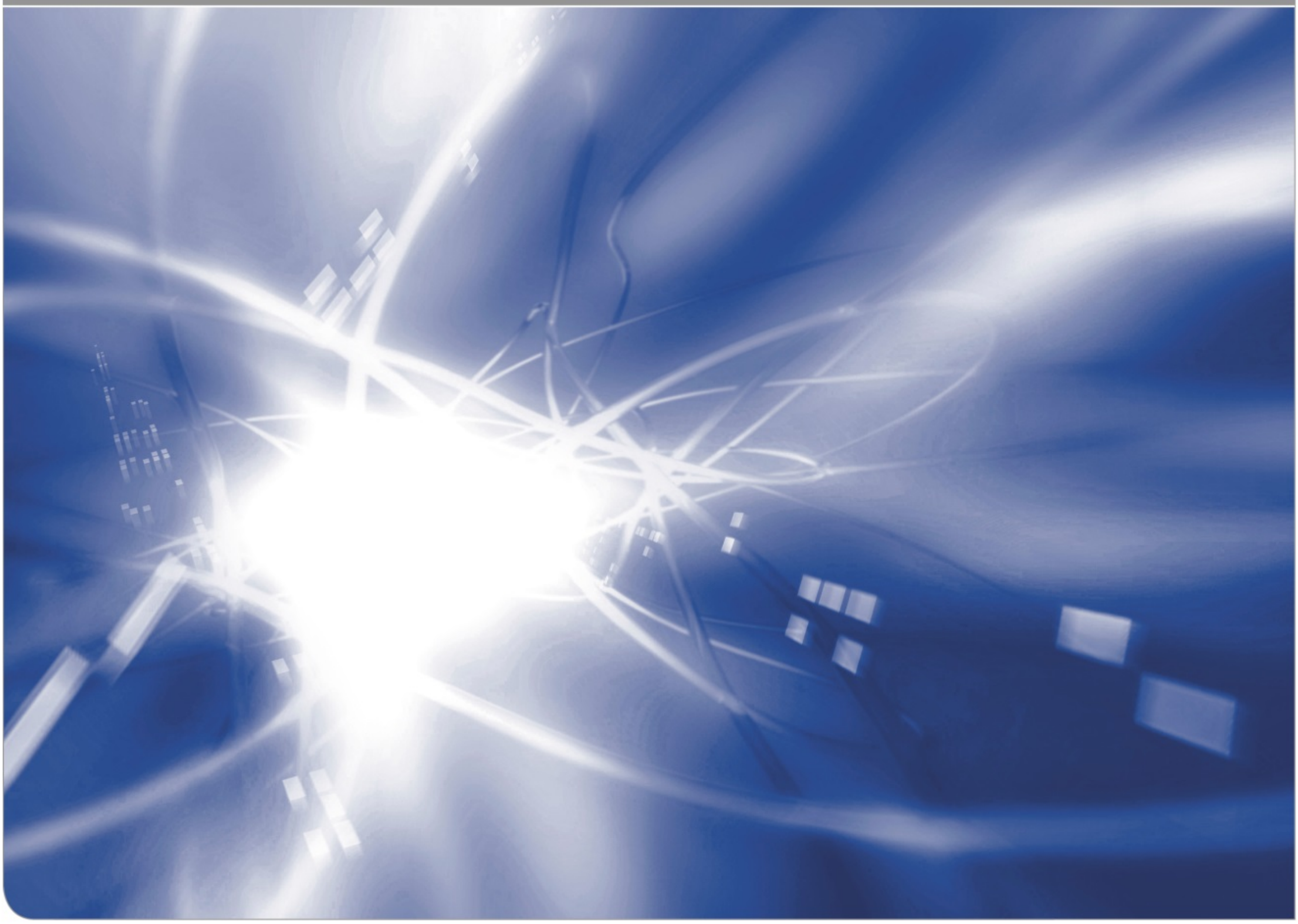

**IAM Institute for Applied Materials**

**Impressum**

Karlsruher Institut für Technologie (KIT)
www.kit.edu



2019

ISSN: 2194-1629

## Abstract

Cracks terminating at free surfaces are affected by local stresses in the surface region. The crack front retards under residual compressive stresses compared with the crack contour in the absence of stresses. This effect had been used in [1] for identifying compression in the surface of chemically toughened and ion-exchanged soda-lime glass surfaces. In [2] the same effect was proven for swelling stresses due to the silica/water reaction. In the present report, the stresses in the surface layers are predicted based on results for soda-lime glass. For silica heat-treated in humid environments, compressive stresses in the order of about -130 MPa to -170 MPa are obtained.

# Contents

# 1. Introduction

In earlier papers [1,2] we described a method for the identification of stresses in the surface region by the observation of crack-terminating angles at free surfaces. The procedure was applied to soda-lime glass [1] and silica [2]. We determined the shielding stress intensity factors $K_{sh}$, defined by the externally applied stress intensity factor $K_{appl}$ and the total stress intensity factor $K_{tip}$ governing crack propagation via

$$K_{tip} = K_{appl} + K_{sh} \tag{1}$$

$K_{tip}$ is for spontaneous and stable crack extension identical with the toughness $K_{Ic}$ and was in our rather fast subcritical crack growth tests on silica $K_{tip}$=0.55-0.6 MPa√m. We will use here an average of $K_{tip}$=0.575 MPa√m. In the present report, the stresses in the surface layer, those are responsible for $K_{sh}$, will be estimated.

Figure 1 shows a crack growing from left to right in a bar with residual stresses in thin surface layers. The crack front terminates at the free surface under an angle φ.

If compressive stresses (expansive strains) occur at the surfaces, the actual crack front in a crack growth test under superimposed external load must stay behind (Fig. 1a). In contrast, tensile stresses caused by shrinking effects must result in an advance of the crack (Fig. 1b).

In [2] we determined the shielding stress intensity factors for silica, heat-treated in water and water vapour, as compiled in Table 1.

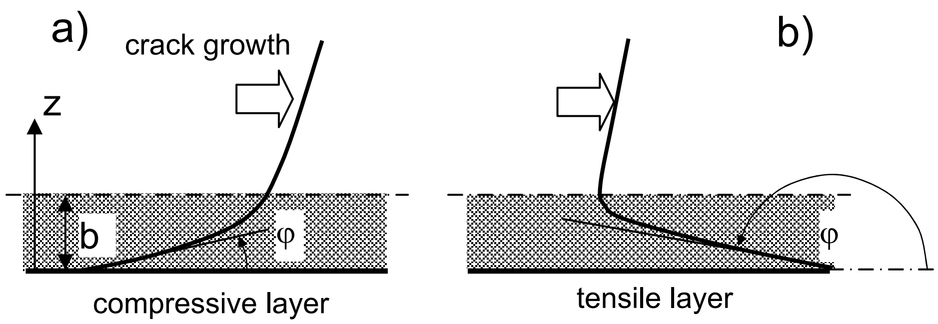


**Fig. 1** Crack fronts terminating at the specimen surface under an angle φ, a) crack retard in a zone of compressive stresses, b) crack advance by tensile stresses. Arrows indicate crack growth direction.

| Treatment | Terminating angle φ | *b*, (µm) | $K_{sh}$ (MPa√m) |
|---|---|---|---|
| 0 h | 83.4° | 0 | 0 |
| 192h $H_2O$-vapour | 25° | 17.7 | −2.37 |
| 48h $H_2O$-liquid | 41.0° | ≈8.9 | −1.20 |
| 192h $H_2O$-liquid | 29.8° | ≈17.7 | −2.64 |

**Table 1** Experimental results for silica, heat-treated at 250°C in water [2], (evaluated for $K_{tip}$=0.57 MPa√m).

The crack-shielding stress intensity factor must be proportional to the swelling stresses $\sigma_{sw}$ acting normal on the crack plane and the square-root of the layer thickness

$$K_{sh} = F(\varphi, b)\sigma_{sw}\sqrt{\pi b} \tag{2}$$

The fracture mechanics geometric function for this loading over a small region, $F(\varphi,b)$, is so far unknown, but may be estimated by not too large effort.

Very often the stresses caused by diffusion processes (here: water diffusion into silica) and the stress distribution is described by

$$\sigma_{sw} = \sigma_{sw,0}\ \mathrm{erfc}\left[\frac{z}{2b}\right] \tag{3}$$

where $\sigma_{sw,0}$ is the surface value, $z$=0, of the stresses and $b$ is the diffusion depth at which the water concentration and consequently the swelling stresses are reduced to ≅50 % of the surface value as is illustrated in Fig. 2a.

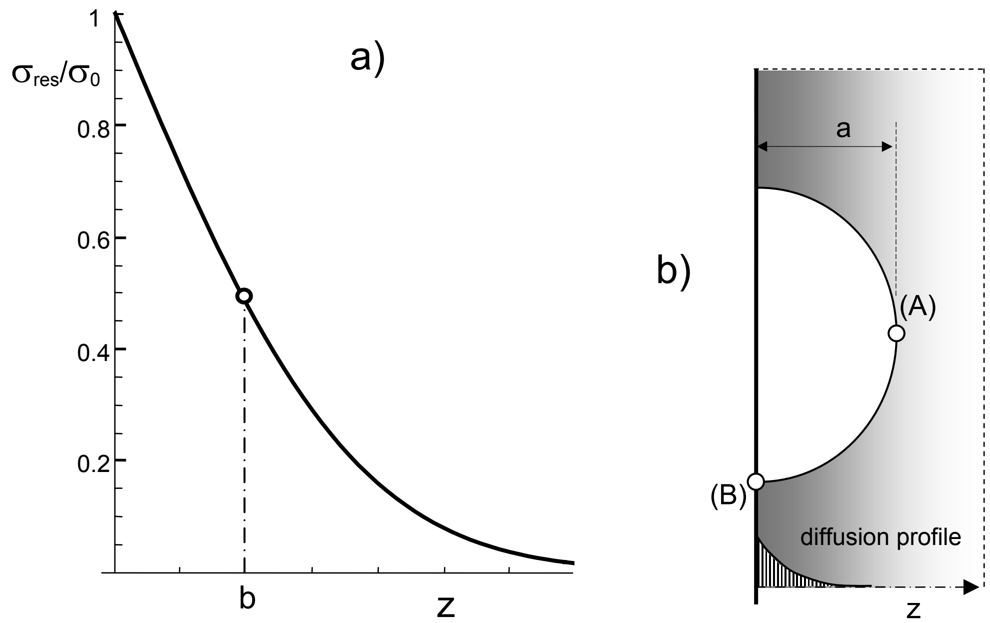


**Fig. 2** a) Stresses in the surface region according to eq.(3), b) semi-circular surface crack loaded by the erfc-shaped stresses.

## 2. Estimation of the magnitude of residual stresses

### 2.1 Stress intensity factor solutions

In order to give an estimation for the maximum swelling stresses in eq.(2) on the basis of the experimentally obtained shielding stress intensity factor, the geometric function $F(\varphi,b)$ must be known.

To the knowledge to the authors, this function is available so far only for the special case of a crack terminating with $\varphi$=90°. For this purpose let us replace the straight crack by a semi-circular surface crack of depth $a$ that might be large compared to the layer thickness, $a \gg b$. The stress intensity factor at the surface point (B), Fig. 2b, from [3] obtained for $b/a > 0.15$ is then

$$K_{sh,B} \cong 1.29\sigma_{sw,0}\sqrt{a}\tanh\left[1.327\sqrt{\frac{b}{a}}+0.064\frac{b}{a}\right] \tag{4a}$$

A series expansion of the FE-results in [3] for $b/a \to 0$ results in the simple expression

$$K_{sh,B} \cong 1.72\sigma_{sw,0}\sqrt{b} \approx \sigma_{sw,0}\sqrt{\pi b} \tag{4b}$$

For the estimation of a solution for crack terminating under the angle $\varphi \neq 90°$, an approximation procedure may be applied.

Finite-Element computations from [1, 2] for silica with Poisson's ratio $\nu=0.17$, are represented in Fig. 3a for crack-terminating angles of $\varphi=45°$, 60°, 83.4°, and 90° in form of the fracture mechanics geometric function $F$, defined for the DCDC-test by

$$F = \frac{K}{|p|\sqrt{\pi R}} \tag{5}$$

In (5) $p$ is the pressure at the end surfaces and $R$ is the radius of the drill hole. The FE-results are introduced as the circles.

For the applied stress intensity factor $K_{appl}(\varphi)$, the result of [2] may be applied that reads for $\nu=0.17$ (silica)

$$\frac{K_{appl}(\varphi)}{K_{appl}(90°)} \cong \frac{1}{0.00658\,\varphi + 7.66\times10^{-13}\,\varphi^6} \tag{6}$$

and for $\nu=0.225$ (soda-lime glass)

$$\frac{K_{appl}(\varphi)}{K_{appl}(90°)} \cong \frac{1}{0.00606\,\varphi + 8.54\times10^{-13}\,\varphi^6} \tag{7}$$

These dependencies are shown in Fig. 3b as the curves together with the data points for $\nu=0.17$ as the circles.

## 2.2 Estimation of the swelling stress in silica

When $F_{appl}(\varphi)$ is the geometric function for the applied stresses, which do not vary over the specimen width $2B$, a rough but frequently used estimation is according to [4]

$$K_{sh}(\varphi,b) = \alpha\, K_{sh}(90°,b) \tag{8a}$$

where the coefficient $\alpha$ is the ratio of the stress intensity factors for the same cracks under a deviating load, here the externally applied load

$$\alpha = \frac{K_{appl}(\varphi)}{K_{appl}(90°)} \tag{8b}$$

However, this procedure can yield larger errors if the shapes of the two cracks to be compared are significantly different. In the original paper by Underwood [4] it was shown that the stress intensity factors for complicated cracks (semi-elliptical surface cracks in thick-walled tubes) under complicated stresses (tension and bending superimposed) were always smaller than those for the reference crack (continuous crack in a plate under pure tension), compare e.g. Fig. 6 in [4]. From this special result of [1] where the actual and the reference case are not very different, we can conclude $\lambda \approx 2/3$. This fact may be indicated by the parameter $\lambda \leq 1$ in (8). The equal sign, $\lambda = 1$, trivially holds when the crack to be predicted is identical with the reference case.

Keeping this fact in mind, we will use the Underwood procedure only for limit case considerations via

$$K_{sh}(\varphi, b) = \lambda \frac{K_{appl}(\varphi)}{K_{appl}(90°)} K_{sh}(90°, b) \quad , \quad \lambda \leq 1 \tag{8c}$$

Since all quantities on the right side of eq.(8c) are known, the shielding stress intensity factor $K_{sh}(\varphi, b)$ can be obtained for silica:

$$K_{sh}(\varphi, b) = \lambda \frac{1}{0.00658\,\varphi + 7.66 \times 10^{-13}\,\varphi^6} \sigma_{sw,0} \sqrt{\pi b} \tag{9}$$

from which the sign and the magnitude of order of swelling stress $\sigma_{sw,0}$ can be estimated by setting $\lambda = 1$.

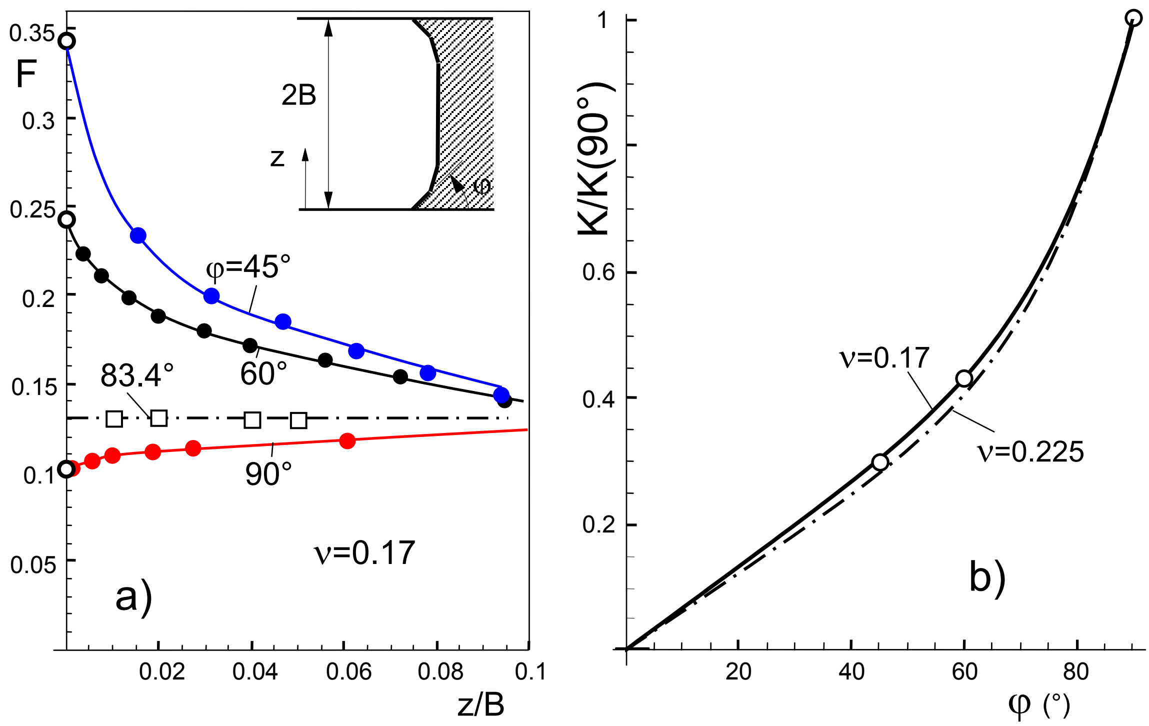


**Fig. 3** Applied stress intensity factors at the surface region of cracks terminating under different angles φ in terms of the geometric function *F* according to eq.(2).

The results for $K_{sh}$ in Table 1, obtained in [2], shall be used here to estimate at least the order of magnitude of the residual stresses from eq.(9). The data in the last Column of Table 2 were derived.

From this result, we can conclude that the surface contains *compressive* stresses stronger than 70 MPa, i.e. $\lambda\times\sigma=-70$ MPa.

| Treatment | $b$, (μm) | $K_{sh}$ (MPa√m) | $\lambda\sigma_{sw}$ (MPa) |
|---|---|---|---|
| 0 h | 0 | 0 | 0 |
| 192h $H_2O$-vapour | 17.7 | −2.37 | −52.4 |
| 48h $H_2O$-liquid | ≈8.9 | −1.20 | −62.1 |
| 192h $H_2O$-liquid | ≈17.7 | −2.64 | −69.7 |

**Table 2** Estimates of swelling stresses, $\sigma_{sw}$.

### 2.3 Residual stresses in soda-lime glass

In the same way as done for silica, let us compute shielding stress intensity factors and residual stresses for the tests on soda-lime glass from [1]. In the tests by Haranoh et al. [5] and Schell et al. [1], crack extension is governed by $K_{tip}=K_{Ic}$. Fracture toughness of soda-lime glass is according to Wiederhorn [6]: $K_{Ic}$=0.75 MPa√m and Poisson's ratio $\nu$=0.225.

In the test in [5] the angle for the untreated test was about $\varphi_0$=90° and in the tests by Schell et al. [1], $\varphi_0$=107°. Consequently,

$$K_{appl}(\varphi_0)=K_{Ic} \tag{10}$$

From eq.(7) it follows for the applied stress intensity factor of the crack-terminating angle $\varphi$

$$K_{sh}(\varphi,b)=\lambda\frac{1}{0.00606\,\varphi+8.54\times10^{-13}\,\varphi^6}\sigma_{sw,0}\sqrt{\pi b}$$

$$\frac{K_{appl}(\varphi)}{K_{appl}(\varphi_0)}=\frac{K_{appl}(\varphi)}{K_{Ic}}\cong\frac{0.00606\,\varphi_0+8.54\times10^{-13}\,\varphi_0^6}{0.00606\,\varphi+8.54\times10^{-13}\,\varphi^6}\overset{def}{=}g(\varphi,\varphi_0) \tag{11}$$

defining the function $g(\varphi,\varphi_0)$ for a shorter notation. Consequently

$$K_{appl}(\varphi)=K_{Ic}\;g(\varphi,\varphi_0) \tag{11a}$$

Then the shielding stress intensity factor becomes

$$\frac{K_{Ic}-K_{sh}(\varphi)}{K_{Ic}}\cong g(\varphi,\varphi_0)\;\Rightarrow\quad K_{sh}(\varphi)=K_{Ic}[1-g(\varphi,\varphi_0)] \tag{12}$$

The terminating angles for the surface-treated tests are compiled in Column 4 of Table 3. The applied and shielding stress intensity factors are given in Columns 5, 6, and the stress estimations in Column 7.

| Treatment | $b$, (μm) | $\varphi_0$ | $\varphi$ | $K_{appl}$ (MPa√m) | $K_{sh}$ (MPa√m) | $\lambda\sigma_{res}$ (MPa) |
|---|---|---|---|---|---|---|
| 0 h | 0 | ≈90° | | 0.75 | 0 | 0 |
| Chem. toughened [5] | 5 | | 13.5° | 9.16 | -8.41 | -174 |
| Ion exchange 0 h [1] | 0 | 107° | | 0.75 | 0 | 0 |
| 1 week | 0.34 | | 71° | 2.68 | -1.93 | -1009. |
| 5 weeks | 0.52 | | 43° | 5.44 | -4.69 | -976. |
| 6 weeks | 0.52 | | 45° | 5.17 | -4.42 | -968. |

**Table 3** Estimates of residual stresses in soda-lime glass [1].

## 3. Discussion of stresses

All residual stresses in Tables 2 and 3 were found to be negative indicating that the water/silica reaction, the ion exchange, and chemical toughening are accompanied by volume expansion. The absolute values of the compressive stresses resulting by the extension of the Underwood procedure depend on the coefficient λ that is not yet known. As can be concluded from Underwood [4], the value of λ decreases with increasing deviation for the reference crack. A rough estimation of λ as a function of φ may be suggested on the basis of soda-lime glass undergoing ion-exchange.

In [7] the stresses by ion exchange were concluded from strength measurements as $\sigma_{res}$=–2425 MPa. A theoretical value of –2300 MPa was determined in [7, 8] for the volume change by the ion-exchange fully transformed in stresses. As an average value, $\sigma_{res}$=–2.4 GPa may be used to compute the value of λ. From the data of $-\lambda\sigma_{res}$ in the last Column of Table 3 and the related terminating angles φ, $\varphi_0$, the red circles in Fig. 4 were obtained. In this plot, the terminating angles φ were normalized on φ=90° representing the reference case (black circle).

The solid curve represents a simple quadratic fit based on the results for the soda-lime glass with the "weight" for the 1-week result (in parentheses) reduced

$$\lambda(\varphi) \cong \tfrac{1}{2}\frac{\varphi}{90°}\left(1+\frac{\varphi}{90°}\right) \tag{13}$$

In the case of swelling stresses in silica, the surface stresses at θ=250°C can be computed from the hydroxyl concentration at the free surface as shown in [9]. The swelling stress components in the surface plane are

$$\sigma_{sw,x} = \sigma_{sw,y} = \tfrac{3}{2}\frac{13.75\,\mathrm{MPa}\,\exp(0.00868\,\theta)}{\tfrac{1}{2}+\tfrac{1}{A}\exp(Q/RT)} \tag{14}$$

with $A$=32.3 and $Q$=10.75 kJ/mol, $T$=θ+273°.

For 250°C eq.(14) yields: –209 MPa. The results for silica predicted with eq.(13) are introduced in Fig. 4 by the blue circles and in Column 3 of Table 4, showing compressive stresses in the range of -130 MPa to -170 MPa.

Applying the relation (13) on the chemically toughened soda-lime glass gives a residual stress of $\sigma_{res}$=–1980 MPa. This result is in agreement with a surface stress of "more than –1000 MPa" as had been reported by Haranoh et al. [5].

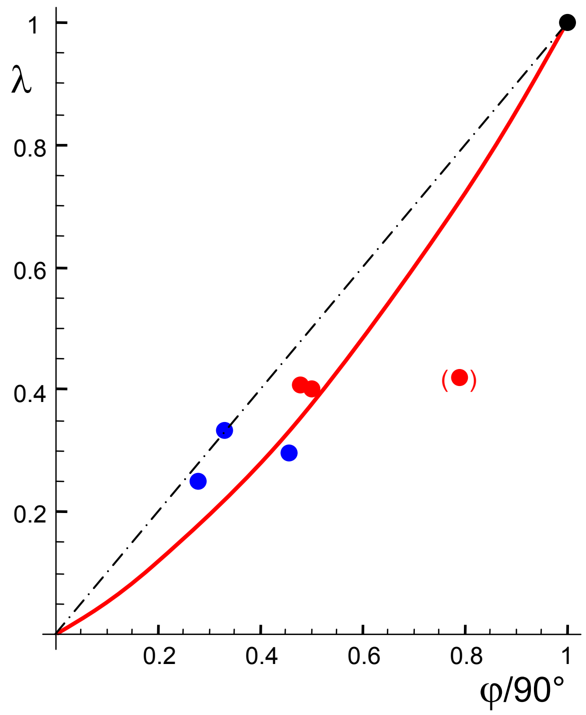


**Fig. 4** Coefficient λ of eq.(8b) as a function of the crack-terminating angle φ; red circles: results for soda-lime glass, red line: related fitting curve for reduced weight of the data point at φ=71° (in parentheses); blue circles: results for silica.

| Material | $\lambda\sigma_{res}$ (MPa) | $\sigma_{res}$ (MPa) |
|---|---|---|
| Chemically toughened *soda-lime* glass [5] | -174 | -1980 |
| *Silica* | | |
| 192h $H_2O$-vapour | -52.4 | -128 |
| 48h $H_2O$-liquid | -62.1 | -151 |
| 192h $H_2O$-liquid | -69.7 | -170 |

**Table 4** Predicted residual stresses for silica and chemically toughened soda-lime glass by use of eq.(13).

## References


1 K.G. Schell, S. Wagner, P. Hettich, T. Fett, G. Rizzi, M.J. Hoffmann, Identification of residual stress layers at glass surfaces via crack terminating angles, *J. Am. Ceram. Soc.* **100**(2017), 4173-4179.
2 P. Hettich, K. G. Schell, G. Rizzi, S. Wagner, T. Fett, Evaluation of crack-terminating angles in heat-treated silica DCDC-specimens, Scientific Working Paper, SWP **114,** 2019, ISSN: 2194-1629, Karlsruhe, KIT.
3 T. Fett, G. Rizzi, M. Hoffmann, S. Wagner, and S.M. Wiederhorn, "Effect of Water on the inert Strength of Silica Glass: Role of Water Penetration," *J. Am. Ceram. Soc.* **95** (2012) [12], 3847-3853..
4 H.J. Underwood, Stress intensity factors for internally pressurized thick-wall cylinders, ASTM STP **53**(1972), 59.
5 T. Haranoh, H. Ishikawa, N. Shinkai, M. Mizuhashi, Crack evolution in Vickers indentation for soda-lime-silica glass, J. of Mater. Science **17**(1982) 1493-1500.
6 S.M. Wiederhorn, "Fracture Surface Energy of Glass," *J. Am. Ceram. Soc.* **52** [2] 99-105 (1969).
7 T. Fett, J.P. Guin, S.M. Wiederhorn, Stresses in ion-exchange layers of soda-lime-silicate glass, Fatigue Fract. Engng. Mater. Struct **28**(2005), 507-514.
8 J.P. Guin, S.M. Wiederhorn, T. Fett, Crack-tip structure in soda-lime-silicate glass J. Am. Ceram. Soc. **88**(2005), 652-59.
9 T. Fett, K.G. Schell, Elimination of swelling stresses from measurements of the equilibrium constant in silica, Scientific Working Paper, SWP **117**, 2019, ISSN: 2194-1629, Karlsruhe, KIT.

KIT Scientific Working Papers
ISSN 2194-1629